

DETC2007-34299

A CONCEPT FOR A MATERIAL THAT SOFTENS WITH FREQUENCY

Jitendra Prasad

Mechanical Engineering Department
Michigan State University
East Lansing MI 48824 USA

Alejandro R. Diaz

Mechanical Engineering Department
Michigan State University
East Lansing MI 48824 USA

ABSTRACT

This work presents design concepts to synthesize composite materials with special dynamic properties, namely, materials that soften at high frequencies. Such dynamic properties are achieved through the use of a two-phase material that has inclusions of a viscoelastic material of negative elastic modulus in a typical matrix phase that has a positive elastic modulus. A possible realization of the negative stiffness inclusion phase is presented. A numerical homogenization technique is used to compute the average viscoelastic properties of the composite. The method and the properties of a composite material designed with it are demonstrated through an example.

1. INTRODUCTION

In applications where vibration suppression is important it is common to use a viscoelastic material such as rubber to reduce the forces transmitted from a vibrating device to its supporting structure. In such applications, at low frequencies small displacements are typically required for good performance and therefore a stiff material is better. However, as the frequency of the excitation increases, the force transmitted to the supporting structure also increases. Since high forces can damage the supporting structure, a *soft* material is better at high frequencies. Thus, in the ideal vibration isolation material, the material stiffness should be a function of the frequency of excitation, stiff at low frequencies but softer at higher frequencies. Unfortunately, typical homogeneous materials actually *harden* at high frequencies. This is true also for composites. For example, a composite made of layers of two or more homogeneous materials will soften only if at least one of the constituents softens with frequency. Such softening will *not* occur if the layers are made of a regular, elastic or viscoelastic materials. However, a composite may soften with frequency if one of the constituents has a negative elastic modulus. Of course, such material does not occur naturally, since materials with a negative stiffness will be unstable on their own.

However, at least in theory, an engineered material with negative stiffness can be made stable if it is properly constrained, e.g., by surrounding it by a sufficiently stiff, regular material. This is the basis for the concepts explored here. The objective of this paper is to generate design concepts that can lead to the synthesis of two-phase composites that soften monotonically with forcing frequency, based on the use of negative stiffness constituents. The goal is to expose novel concepts and algorithms that could be used as guidelines by material scientists in future work, rather than to provide a specific recipe to synthesize the material.

The plan is as follows: we shall focus on 2D composites formed by periodic inclusions of one material –material B- into a viscoelastic matrix of a second material, material A. This composite is introduced in section 2.1. Material A is standard, but material B has some elements of negative stiffness. To understand the behavior of such materials, we start with a 1-D model, discussed in section 2.2. We find that to make B stable, its negative stiffness component has to be layered with a regular material. Thus B is itself a composite, a layered mixture of two materials, one unstable (B_1) and the other one stable and “standard” (B_2). This is discussed in section 2.3, where the focus is on the stability of the mixture. Once a possible viscoelastic tensor for B_1 is found, we then relate it to a physical system, a 2D array of springs and dashpots whose overall behavior mimics that of (the just proposed) B_1 . This is discussed in section 2.4. Finally, the properties of the mixture of A and B are computed in section 2.5. There, and throughout the paper, standard methods of periodic homogenization are used to compute the viscoelastic tensor associated with periodic mixtures of two or more constituents. Such methods and related numerics are well established and the interested reader should refer to, e.g., Cioranescu and Donato (2000) for background or to Diaz and Benard (2002) for a succinct description of the practical aspects of such computations. The composite mixture of A and B is the final result. The performance of the designed material is demonstrated through an example in section 3. The paper ends with brief final remarks.

NOMENCLATURE

- ω : The frequency of excitation
- E_1, E_2 : Elastic moduli of a viscoelastic material. Real scalars. Here, $E_2 > 0$ but $E_1 < 0$.
- η : Damping coefficient of a viscoelastic material. A positive, real scalar
- E_{B1}^* : Viscoelastic modulus of a material made up of elastic components of moduli E_1 and E_2 (arranged in series) and damping coefficient η (arranged in parallel with E_2 .) A complex scalar, frequency dependent.
- C_{B1} : The viscoelastic material tensor of an isotropic material B_1 of modulus E_{B1}^* and fixed Poisson's ratio ν . Material B_1 has negative stiffness components. A symmetric, complex, 3x3 matrix in 2D elasticity.
- C_B : The viscoelastic material tensor of a composite material B formed by layering material B_1 with a (standard) viscoelastic material B_2 in the '1' direction. A symmetric, complex, 3x3 matrix in 2D elasticity.
- C_Q : A viscoelastic material tensor that numerically approximates C_{B1} and can be achieved by a discrete physical arrangement of springs and dampers. A symmetric, complex, 3x3 matrix in 2D elasticity.
- C_H^* : The viscoelastic tensor of a composite mixture of a matrix A (a standard viscoelastic material) with an inclusion of material B. A symmetric, complex, 3x3 matrix in 2D elasticity.

2. METHODOLOGY

2.1 Two Phase Composite Material

The strategy relies on the study of composite materials with a periodic micro-structure. In particular, we study a two-phase composite composed of periodic inclusions of a viscoelastic phase B in an elastic or viscoelastic matrix A. A schematic arrangement of such composites is shown in Fig. 1. The dashed square in Fig. 1 shows a fundamental cell of the periodic arrangement. The properties of A and B and the shape of the inclusion are the variables to be adjusted so that the composite softens with increasing forcing frequency. The matrix A could be any typical material, e.g., rubber. The inclusion B will be made up of two distinct isotropic phases, B_1 and B_2 . Material B_1 will be allowed to have negative stiffness, while material B_2 is again a standard material, e.g., rubber. The reasons for this particular choice for the inclusion material B are explained in the following sections.

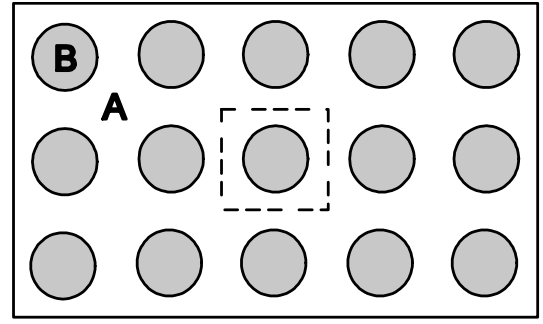


Figure 1. A two-phase periodic composite material. Dashed box shows the fundamental cell.

2.2 Negative Stiffness Phase (B_1)

A negative stiffness material has a negative elastic modulus. Such materials are not stable and therefore they do not remain in a negative stiffness state. However, it is known (e.g., see Lakes and Drugan (2002)) that a block of material of negative stiffness can be made stable by surrounding it with a typical (i.e. stable) material. Negative stiffness materials are realizable. A typical way to implement negative stiffness is through the use of bistable structures, positioned in their unstable configuration and held there by surrounding, stable material (see Prasad and Diaz (2005, 2006)). Lakes and Drugan (2002) and Wang and Lakes (2004b, 2005) show how lumped structures can be used to implement negative stiffness inclusions.

A material B_1 with negative stiffness is modeled here as a standard linear solid. Such model of viscoelasticity is sketched in Fig. 2, where E_1 , E_2 and η are the three parameters of the standard linear solid. In a typical viscoelastic material these parameters are positive. However, in the present case, E_1 is negative, while E_2 and η are positive.

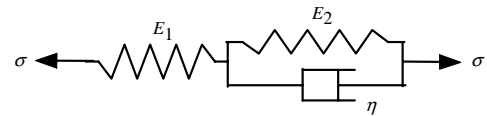


Figure 2. Standard linear solid model of viscoelasticity

The complex modulus that corresponds to the viscoelastic model shown in Fig. 2 is given by

$$E_{B1}^*(\omega) = \frac{E_1(E_2 + i\eta\omega)}{(E_1 + E_2 + i\eta\omega)} \quad (2.2.1)$$

where ω is the forcing frequency. When B_1 is isotropic, the corresponding elastic tensor is given by

$$C_{B1} = \frac{E_{B1}^*}{1 - \nu_{B1}^2} \begin{bmatrix} 1 & \nu_{B1} & 0 \\ \nu_{B1} & 1 & 0 \\ 0 & 0 & (1 - \nu_{B1})/2 \end{bmatrix} \quad (2.2.2)$$

Here ν_{B_1} is the Poisson's ratio. In (2.2.1), E_1 and E_2 are such that the corresponding Young's modulus (i.e., $\text{Re}(E_{B_1}^*(0))$) is negative. Thus, we refer to B_1 as the 'negative stiffness' phase.

2.3 Stability of the Negative Stiffness Phase B_1

A negative stiffness phase B_1 will be unstable because the corresponding shear modulus will be negative (Lakes and Drugan (2002)). For this reason, the negative stiffness phase B_1 cannot be used directly as the inclusion phase B (i.e., if B_1 were inserted directly as the inclusion in matrix A, in general the resulting composite would be unstable). Instead, we must look for a material B that has a negative Young's modulus, to achieve frequency softening, but positive shear modulus, to maintain stability. This can be accomplished by layering B_1 with a regular material, B_2 .

In order to avoid loss of stability, a model for B is proposed, whereby B is itself a mixture of two isotropic constituents, B_1 and B_2 . In this model, the constituent with negative stiffness (B_1) is always surrounded by a second phase of stable material (B_2). One such arrangement is shown in Fig. 3. The resulting effective properties of B correspond to a "rank 1" layering of B_1 and B_2 along the horizontal direction (direction 1). The effective elastic tensor for phase B is computed using well known layering formulas:

$$b_{11}(\omega) = \frac{q_{11}r_{11}}{(1-g)r_{11} + gq_{11}} \quad (2.3.1)$$

$$b_{12}(\omega) = \left(g \frac{r_{12}}{r_{11}} + (1-g) \frac{q_{12}}{q_{11}} \right) b_{11}(\omega) \quad (2.3.2)$$

$$b_{22}(\omega) = (gr_{22} + (1-g)q_{22}) - \left(g \frac{r_{12}^2}{r_{11}} + (1-g) \frac{q_{12}^2}{q_{11}} \right) + \frac{(b_{12}(\omega))^2}{b_{11}(\omega)} \quad (2.3.3)$$

$$b_{33}(\omega) = \frac{q_{33}r_{33}}{(1-g)r_{33} + gq_{33}} \quad (2.3.4)$$

where q_{ij} and r_{ij} are the ij -components of the elastic tensors (C_{B_1} and C_{B_2}) for phases B_1 and B_2 , respectively. g is the volume fraction of B_2 in B. The effective elastic tensor is given by

$$C_B = \begin{bmatrix} b_{11}(\omega) & b_{12}(\omega) & 0 \\ b_{12}(\omega) & b_{22}(\omega) & 0 \\ 0 & 0 & b_{33}(\omega) \end{bmatrix} \quad (2.3.5)$$

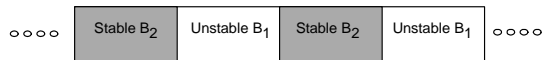


Figure 3. A potential arrangement of constituents B_1 and B_2 to form material B

With suitable values for the free parameters g , C_{B_1} and C_{B_2} , the layered set up can result in an elastic tensor for B where the 2-2 entry (C_{2222}) is negative, to produce frequency induced softening, while the 3-3 entry (C_{1212}) is positive, to make stability possible when B is inserted in A. The choice of B_2 is somewhat arbitrary (as long as it is a standard material). We choose both A and B_2 to be the same material.

2.4 A Lumped System Realization of Material B

One way to visualize the behavior and inner-workings of B_1 is to use an arrangement of springs and dampers where some of the springs have negative stiffness. Negative stiffness may be realized using e.g., bistable structures, as shown in Prasad and Diaz (2005, 2006). Figure 4 shows a potential configuration. As shown in the figure, the structure is a four-noded square, with two degrees of freedom at each node. The nonlinear springs in the figure (shown as springs with an arrow across) correspond to bistable structures that can be used to provide the desired negative stiffness. Material B_1 is obtained by tiling a plane with the two dimensional lattice shown in Fig. 4.

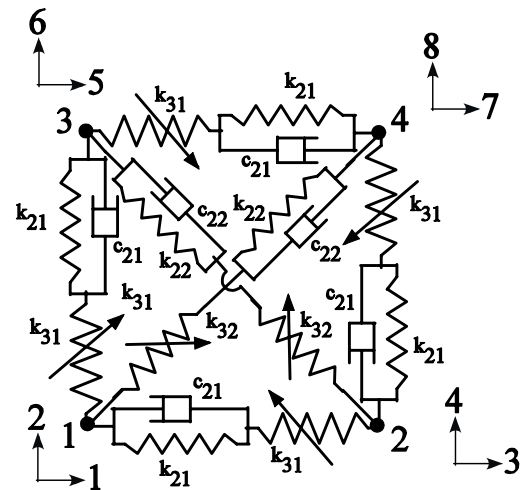


Figure 4. Two-dimensional lattice of phase B_1

The 2D lattice in Fig. 4 is basically made up of 6 standard linear solid (SLS) elements interconnecting the 4 nodes. k_{ij} and c_{ij} in the figure denote spring stiffness and damper coefficient, respectively. The complex stiffness of each of the four identical SLS elements forming the four sides of the lattice is given by

$$s_1 = \frac{k_{31}(k_{21} + i\omega c_{21})}{k_{31} + k_{21} + i\omega c_{21}} \quad (2.4.1)$$

Similarly, the complex stiffness of either of the two identical SLS elements forming the two diagonals of the lattice is given by

$$s_2 = \frac{k_{32}(k_{22} + i\omega c_{22})}{k_{32} + k_{22} + i\omega c_{22}} \quad (2.4.2)$$

The complex stiffness matrix (K_Q^*) for the 2D element in Fig. 4 is given by

$$K_Q^* = \begin{bmatrix} s_1 + \frac{s_2}{2} & \frac{s_2}{2} & -s_1 & 0 & 0 & 0 & -\frac{s_2}{2} & -\frac{s_2}{2} \\ \frac{s_2}{2} & s_1 + \frac{s_2}{2} & 0 & 0 & 0 & -s_1 & -\frac{s_2}{2} & -\frac{s_2}{2} \\ -s_1 & 0 & s_1 + \frac{s_2}{2} & -\frac{s_2}{2} & -\frac{s_2}{2} & \frac{s_2}{2} & 0 & 0 \\ 0 & 0 & -\frac{s_2}{2} & s_1 + \frac{s_2}{2} & \frac{s_2}{2} & -\frac{s_2}{2} & 0 & -s_1 \\ 0 & 0 & -\frac{s_2}{2} & \frac{s_2}{2} & s_1 + \frac{s_2}{2} & -\frac{s_2}{2} & -s_1 & 0 \\ 0 & -s_1 & \frac{s_2}{2} & -\frac{s_2}{2} & -\frac{s_2}{2} & s_1 + \frac{s_2}{2} & 0 & 0 \\ -\frac{s_2}{2} & -\frac{s_2}{2} & 0 & 0 & -s_1 & 0 & s_1 + \frac{s_2}{2} & \frac{s_2}{2} \\ -\frac{s_2}{2} & -\frac{s_2}{2} & 0 & -s_1 & 0 & 0 & \frac{s_2}{2} & s_1 + \frac{s_2}{2} \end{bmatrix} \quad (2.4.3)$$

The complex modulus tensor (C_Q) corresponding to the arrangement in Fig. 4 is of the form:

$$C_Q = \begin{bmatrix} f_{11} & f_{12} & 0 \\ f_{12} & f_{11} & 0 \\ 0 & 0 & f_{33} \end{bmatrix} \quad (2.4.4)$$

Three numerical tests are conducted to find C_Q :

(i) **Tension test 1:** Degrees of freedom 1, 2, 3, 4, 5 and 7 are constrained (zero prescribed displacement) and degrees of freedom 6 and 8 are given unit displacements. f_{11} is the total reaction force along the degrees of freedom 6 and 8. f_{11} is given by

$$f_{11} = 2s_1 + s_2 \quad (2.4.5)$$

(ii) **Tension test 2:** Degrees of freedom 1, 2, 3, 4, 5 and 7 are constrained (zero prescribed displacement) and degrees of freedom 6 and 8 are given unit displacements. f_{12} is the total reaction force along the degrees of freedom 1 and 5. f_{12} is given by

$$f_{12} = s_2 \quad (2.4.6)$$

(iii) **Shear test:** Degrees of freedom 1, 2, 3, 4, 6 and 8 are constrained (zero prescribed displacement) and degrees of freedom 5 and 7 are given unit displacements. f_{33} is the total reaction force along the degrees of freedom 5 and 7. f_{33} is given by

$$f_{33} = s_2 \quad (2.4.7)$$

Our aim is to construct an isotropic material using the structure in Fig. 4. In other words, we want to express C_Q in the form of (2.2.2). This is possible if

$$s_1 = s_2 \quad (2.4.8)$$

$$E_{B1}^* = \frac{8s_1}{3} = \frac{8s_2}{3} \quad (2.4.9)$$

and

$$\nu_{B1} = \frac{1}{3} \quad (2.4.10)$$

As an example (to be used in section 3), we choose the following parameters:

$$\begin{aligned} k_{21} &= 8.45E_{A1} \\ k_{31} &= -0.304k_{21} \\ c_{21}/k_{21} &= 0.0002 \\ k_{22} &= k_{21} \\ k_{32} &= k_{31} \\ c_{22} &= c_{21} \end{aligned}$$

The corresponding elastic tensor is C_{B1} in (2.2.2) with

$$E_{B1}^* = -\frac{6.8501(1+i0.0002\omega)}{0.696+i0.0002\omega} E_{A1}$$

and $\nu_{B1} = 1/3$.

Note that while it may be possible to synthesize a lumped model for phase B directly (by-passing the construction of B_1 followed by layering), finding a lumped model with the desired properties may be difficult.

2.5 Homogenization of Viscoelastic Properties

With phases A and B in hand, the final step is to compute the effective properties of the mixture of A and B, e.g., characterized by a simple arrangement such as that in Fig. 5. This can be accomplished by numerical homogenization (notice that this suggests that the mixture of constituents B_1 and B_2 takes place at a smaller scale than the mixture of A and B). The representative cell is discretized using standard, 2D quadrilateral finite elements and the effective properties of the mixture are obtained by exposing the cell to three states of (unit) pre-strain, as is standard in numerical homogenization methods (details can be found in Yi et. al. (2000)). The computed homogenized elastic tensor of the composite material has the information of whether the composite material softens with frequency. In particular, a monotonic decrease in the absolute value of the second diagonal entry of the effective tensor indicates softening of the composite material in direction 2.

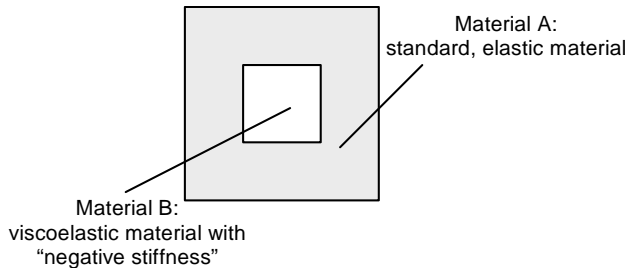


Figure 5. Representative cell characterizing the (periodic) mixture of materials A and B

3. EXAMPLE

Here we will illustrate the properties of a material constructed as described above using a numerical example. We first select a typical rubber-like viscoelastic material for phases A and B₂. The (complex) elastic tensor of phase A is

$$C_A = C_A^0(1 + i\delta_A) \text{ with } C_A^0 = \frac{E_A}{1 - \nu_A^2} \begin{bmatrix} 1 & \nu_A & 0 \\ \nu_A & 1 & 0 \\ 0 & 0 & (1 - \nu_A)/2 \end{bmatrix}$$

where Young's modulus E_A is arbitrary but real and positive and Poisson's ratio $\nu_A = 0.45$. The structural damping coefficient δ_A is 0.07. As indicated, we use this material also in phase B₂ of B, i.e., $C_{B2} = C_A$.

Phase B is a layered material. Here phase B is constructed by alternating layers of B₂ and a negative-stiffness material B₁. The volume fraction of B₂ in B is 0.8.

Phase B₁ is made of a material such as the spring-damper structure shown in Fig. 4. Its elastic tensor is as in (2.2.2) with $\nu_{B1} = 1/3$ and

$$E_{B1}^* = -\frac{6.8501(1 + i0.0002\omega)}{0.696 + i0.0002\omega} E_A$$

The values of E_{B1}^* and ν_{B1} used here correspond to the example material B₁ computed in section 2.4.

The final mixture corresponds to the periodic mixture of phases A and B characterized by the periodic repetition of the cell in Fig. 5. The volume fraction of phase B is 16%. The unit cell is discretized into 50x50 square plane stress elements for numerical analysis. The resulting homogenized complex modulus tensor of the two-dimensional composite is given by

$$C_H^* = \begin{bmatrix} c_{11}(\omega) & c_{12}(\omega) & 0 \\ c_{12}(\omega) & c_{22}(\omega) & 0 \\ 0 & 0 & c_{33}(\omega) \end{bmatrix}$$

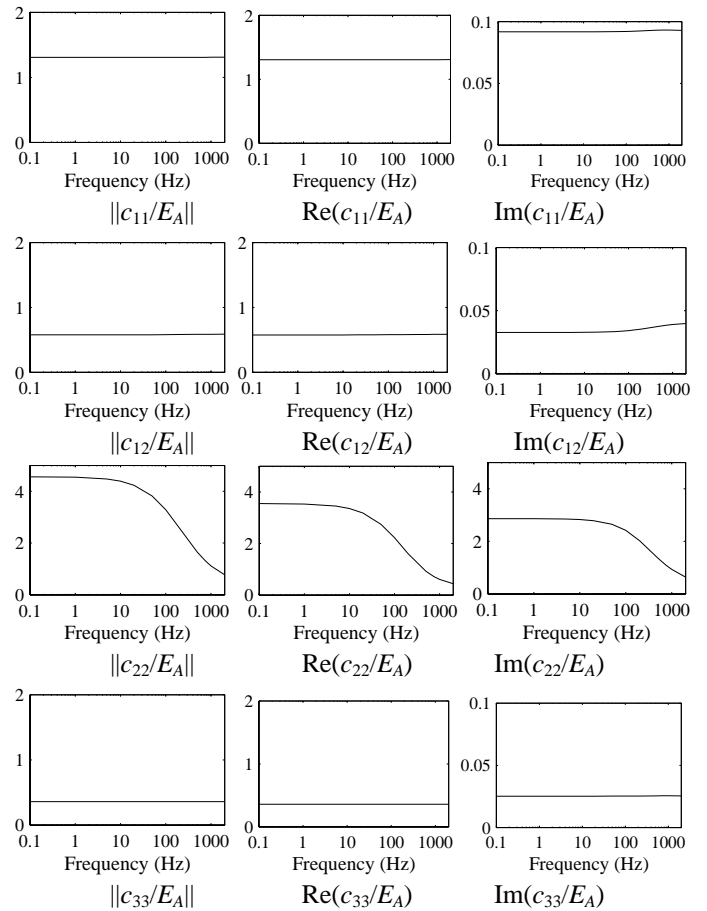


Figure 6. Components of the effective elastic tensor after mixing A and B

The absolute values, real and imaginary parts of $c_{ij}(\omega)$ are plotted versus the forcing frequency in Fig. 6. $c_{ij}(\omega)$ values are normalized by E_A .

As can be seen in Fig. 6, $\|c_{22}(\omega)\|$ decreases with forcing frequency ω , while $\|c_{11}(\omega)\|$, $\|c_{12}(\omega)\|$ and $\|c_{33}(\omega)\|$ are almost constant. This implies that frequency-induced softening is achieved if the composite material is loaded in direction 2 while the material is constrained in direction 1. Direction 1 is along the thickness of the layers (of phase B₁ or B₂) inside phase B, as shown in Fig. 7. Frequency-induced softening of the dynamic modulus is achieved under unidirectional loading – when the composite material is loaded in direction 2.

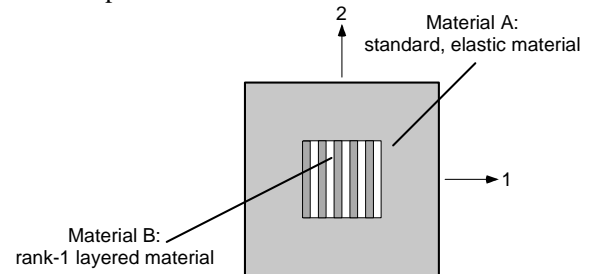


Figure 7. Phase B as layered material

3.1 Transmissibility Analysis

Now we will demonstrate the vibration isolation performance of the material designed in this example. We use a cylindrical block of the composite material synthesized here as a vibration-isolation device, and carry out a transmissibility analysis. Figure 8 shows the vibration-isolation device. The cross-sectional area of the cylinder is a (i.e. the radius of the cylinder is $\sqrt{a/\pi}$). The device supports a mass m and the unbalanced disturbance force acting on the mass is F . F_s is the force transmitted to the structure. The transmissibility of the system is $T = \|F_s\| / \|F\|$. An effective vibration isolation performance corresponds to low transmissibility.

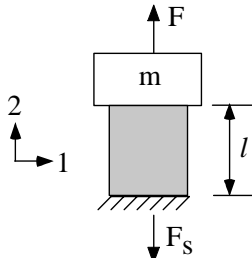


Figure 8. Vibration-isolation system

The components of the elastic tensor of the composite material used to build the vibration-isolation device are those plotted in Fig. 6. In Fig. 8, the vibration-isolation device is unidirectionally loaded in direction 2 and it is not constrained in direction 1. As indicated earlier in this section, direction 2 is perpendicular to the layering direction, as shown in Fig. 7. Under the given boundary condition the strain (ϵ_{22}) and the stress (σ_{22}) in direction 2 are related as

$$\sigma_{22} = E_C(\omega)\epsilon_{22}$$

where

$$E_C(\omega) = c_{22}(\omega) - \nu(\omega)c_{12}(\omega)$$

and

$$\nu(\omega) = \frac{c_{12}(\omega)}{c_{11}(\omega)}$$

$E_C(\omega)$ and the effective stiffness of the vibration-isolation device $k_C(\omega)$ are related by

$$k_C(\omega) = \frac{E_C(\omega)a}{l}$$

The absolute value, real and imaginary parts of $E_C(\omega)$ are plotted in Fig. 9, where values are normalized by E_A (i.e., the Young's modulus of phase A). It can be seen in the figure that

$\text{Re}(E_C(0))$ is approximately $3E_A$. In other words, the effective Young's modulus of the composite material is $3E_A$. Typically, the static stiffness (i.e., $k_C(0)$) of the vibration-isolation device is prescribed. In this case, suppose $k_C(0)$ is set to 170 N/mm. This stiffness is achieved with, for example, $E_A = 4 \text{ N/mm}^2$, $l = 30 \text{ mm}$ and $a = 425 \text{ mm}^2$.

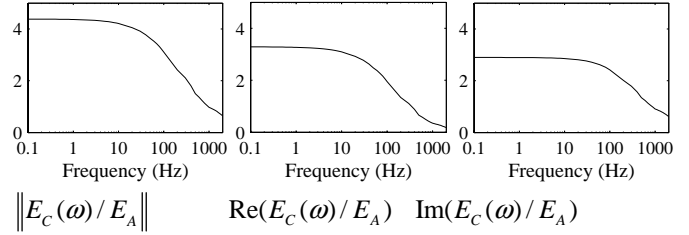


Figure 9. The effective complex modulus $E_C(\omega)$

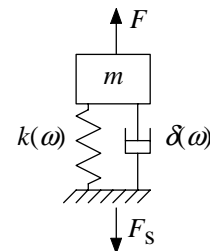


Figure 10. Vibration-isolation device as spring-damper system

The vibration-isolation device in Fig. 8 may be represented as a system of a spring and a damper connected in parallel, as shown in Fig. 10. The corresponding spring stiffness ($k(\omega)$) and the structural damping coefficient ($\delta(\omega)$) are

$$k(\omega) = \text{Re}(k_C(\omega))$$

$$\delta(\omega) = \frac{\text{Im}(k_C(\omega))}{\text{Re}(k_C(\omega))}$$

$k(\omega)$ and $\delta(\omega)$ are plotted in Fig. 11.

Note that the complex stiffness of the vibration-isolation device is $k_C(\omega)$, which is directly proportional to the complex modulus $E_C(\omega)$. As can be seen in Fig. 9, the absolute value, real and imaginary parts of $E_C(\omega)$ decrease monotonically with frequency. This implies that the dynamic stiffness of the vibration-isolation device, $\|k_C(\omega)\|$, and the real and imaginary parts of the complex stiffness ($k(\omega)$ and $\delta(\omega)k(\omega)$, respectively) also decrease monotonically with frequency. However, the effective structural damping coefficient $\delta(\omega)$ increases with frequency, as shown in Fig. 11. The dashed lines in Fig. 11 correspond to $k(\omega)$ and $\delta(\omega)$ of the vibration-isolation device if the device were made of phase A alone.

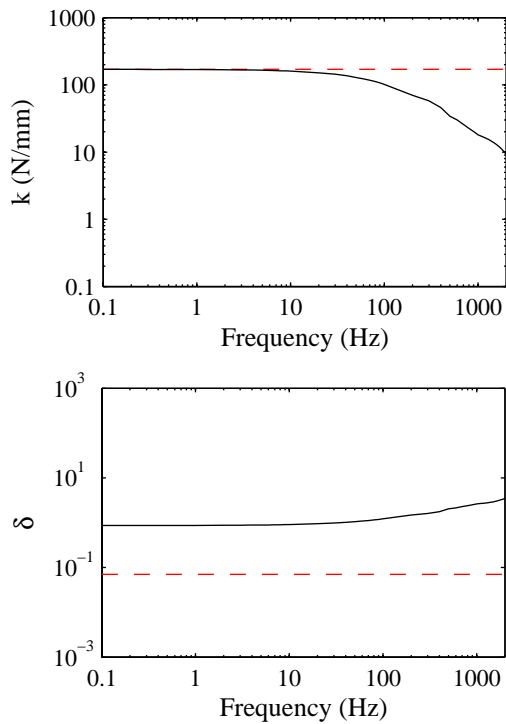


Figure 11. Spring stiffness ($k(\omega)$) and damping coefficient ($\delta(\omega)$) of the vibration-isolation device

With $k(\omega)$ and $\delta(\omega)$ in hand, the next step is to compute the transmissibility of the device, defined here as

$$T(\omega) = \left\| \frac{F_s}{F} \right\| = \left\| \frac{1 + i\delta(\omega)}{1 - m\omega^2 / k(\omega) + i\delta(\omega)} \right\|$$

Note that the above expression for $T(\omega)$ may not be ideal for a nonlinear system where $k(\omega)$ and $\delta(\omega)$ are functions of frequency; however, we use this expression for simplicity as is standard in engineering practice.

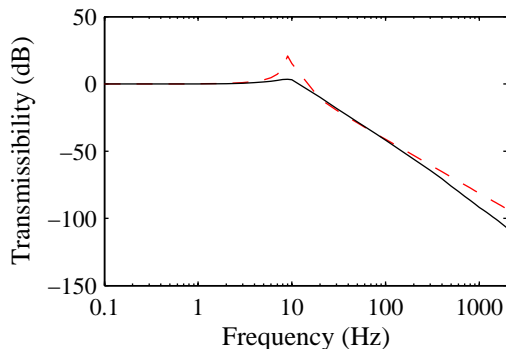


Figure 12. Transmissibility as a function of frequency

The transmissibility $T(\omega)$ is plotted in Fig. 12 (measured in decibels). The solid line corresponds to the composite material, while the dashed line corresponds to phase A alone.

The reduction in transmissibility at low frequencies –near the resonance peak at about 10Hz – is associated with the increased damping of the composite C, when compared to material A alone (as seen in Fig. 11). The reduction in transmissibility at high frequencies, in the 1000 Hz regime, is of several orders of magnitude, suggesting that significant improvements can be achieved by using C, even if unavoidable imperfections and uncertainties in material properties affect the final answer.

FINAL REMARKS

A model of a material that exhibits frequency-induced softening has been proposed. The model is 2-D and based on a periodic mixture of two phases: A (matrix phase) and B (inclusion phase). Simultaneous softening and stability are achievable if phase B itself is a small scale mixture of two constituents, one elastic and the other one with negative stiffness. While the performance of the A-B mixture in terms of frequency-induced softening is better than the performance of A alone, there is still room for improvement through optimization by adjusting the constituent material properties (as well as the shape of the inclusion, as indicated below).

Construction of B by layering will result in a phase B that is not isotropic and therefore mixing A and B may result in a material that is not isotropic either. In practice one may be interested only in isotropic materials and therefore the micro-geometry of the mixture of A and B must be designed so that the mixture is isotropic. While there was no attempt to do this in this work, this can be done by casting the problem as an inverse homogenization problem (as discussed e.g. in Sigmund (1995)). This methodology can be used to tailor the material tensor to desired specifications, by re-adjusting the shape of the inclusion of B inside A.

While the stability of the mixture was verified against *certain* modes of instability, one cannot say for sure that the material is stable with regard to all possible modes of instability. Further analysis may determine that additional conditions may be required. A full answer can be obtained only through experimentation.

The concept presented here is attractive and may provide indications on what avenues to pursue in the future. An attractive direction involves the realization of the negative stiffness inclusion by means of a bistable structure inside the composite. This could be accomplished perhaps by pre-stressing one of the constituents to a post-buckled state.

Acknowledgement

This work was generously supported by Toyota Motor Corporation of Nagoya, Japan, Vehicle Engineering Division. This support is gratefully acknowledged.

REFERENCES

Bensoussan, A., Lions, J.L., and Papanicolau, G., 1978, *Asymptotic Analysis for Periodic Structures*, North-Holland, Amsterdam.

Cioranescu, D and Donato P., An Introduction to Homogenization - Oxford Lecture Series in Mathematics and Its Applications, 17. Oxford University Press, 2000

Diaz, A. R. and Benard, A., 2003, "Designing materials with prescribed elastic properties using polygonal cells," International Journal for Numerical Methods in Engineering, Vol. 57 (3), pp. 301-314.

Lakes, R. S. and Drugan, W. J., 2002, "Dramatically stiffer elastic composite materials due to a negative stiffness phase?", J. Mechanics and Physics of Solids, 50, 979-1009.

Prasad, J., and Diaz, A.R., 2005, "Layout of tileable multistable structures using topology optimization," in Proceedings of TopoptSYMP2005, IUTAM symposium, Rungstedgaard, Copenhagen, Denmark, October 26 – 29, 2005.

Prasad, J. and Diaz, A.R., 2006, "Synthesis of Bistable Periodic Structures Using Topology Optimization and a Genetic Algorithm," Journal of Mechanical Design, Vol. 128, pp. 1298-1306.

Sigmund, O., 1995, "Tailoring materials with prescribed elastic properties," Mechanics of Materials, Vol. 20, pp.351-368.

Wang, Y. C. and Lakes, R. S., 2004a, "Extreme stiffness systems due to negative stiffness elements", American J. of Physics, 72, Jan. (2004).

Wang, Y. C. and Lakes, R. S., 2004b, "Negative stiffness induced extreme viscoelastic mechanical properties: stability and dynamics", Philosophical Magazine, 35, 3785-3801, Dec. (2004).

Wang, Y.C. and Lakes, R. S., 2005, "Composites with inclusions of negative bulk modulus: extreme damping and negative Poisson's ratio," Journal of Composite Materials, Vol. 39 (18), pp. 1645- 1657.

Yi, Y.M., Park, S.H. and Youn, S.K., 2000, "Design of microstructures of viscoelastic composites for optimal damping characteristics," International Journal of Solids and Structures, Vol. 37, pp. 4791-4810.